

Content-based Colour Space

Javier Vazquez i Corral

JVAZQUEZ@CVC.UAB.ES

Computer Vision Centre/Computer Science Department

Building O - Campus UAB, 08193 Bellaterra (Barcelona), Spain

Tutor: Maria Vanrell i Martorell

Abstract

The main goal of this paper is to define a new colour space that represents the colour information of the image in such a way to give a more coherent spatio-chromatic representation. This space can allow to improve the performance of the algorithms of blob detection. To build the space we base colour representation on the ridges of the colour image distribution since it has been proved that they capture the essential colours of the image. Then we will define a colour space where each channel depends on one of the ridges and we explain how we can make an inverse transformation to the original space. Finally, to select the essential channels we suggest three different criteria: one based on a minimization of the mutual information, another based on a distance-maximization and the third one based on high-level hypothesis called nameability.

Keywords: Colour space, nameability, blob detection

1. Introduction

Colour is an important cue for Computer Vision. It is useful in different visual tasks such as segmentation, blob detection and tracking (Cheng et al., 2001). It is also one of the principal advantages of trichromatic primates over other primates. Colour was also an important step in primates evolution, since they became fitter than other primates at the moment they could choose the best coloured fruits using colour vision, leading to the current dominance of trichromatic primates (and humans) in the world.

Evolutionary biology has discussed about this topics a lot of years (Mollon, 1989), (Dominy and Lucas, 2001) and (Parraga C.A. and D.J., 2002) and it also has proved some particularities of the Human Visual System (HVS), for example, colour is useful in shadow removal (Lovell and Troscianko).

It is related to the importance of colour in Computer Vision that our work makes sense. In this work we propose a new colour space that adapt to the image context.

Several colour spaces had been defined in colour science (Wyszecki and Stiles, 1982), each one with a certain intention. Some of them, as RGB or CMY, trying to improve the image acquisition, visualization or printing devices. Others, the uniform spaces, such as, CIELAB or CIELUV, allowing an Euclidean distance to represent perceptual similarity.

This work have a first clear application that we focus on, it is the computational detection of colour image blobs.

Detection of coloured image blobs is a low-level visual task of a great importance in computer vision. In computer vision an image blob is a connected image region presenting an homogeneous colour. A successful extraction of image blobs can be the basis to overcome

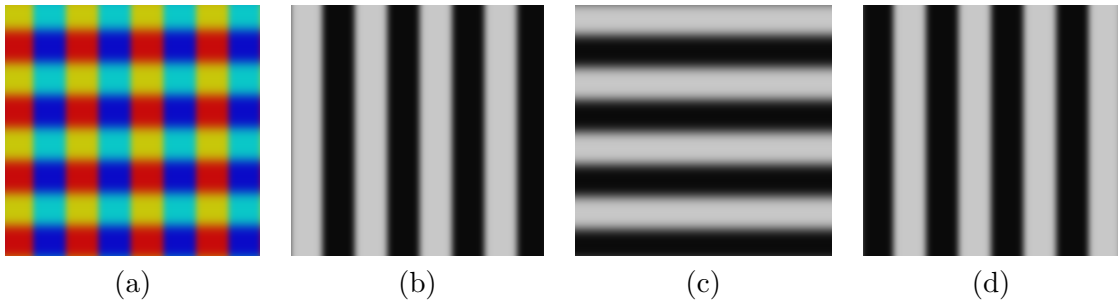


Figure 1: RGB channels of image (a), where (b) is the red channel, (c) the green channel, and (d) the blue channel

the subsequent steps in the image understanding process. Blob extraction is essential in the first steps of texture description (Julesz and Bergen, 1983), background subtraction (Collins et al., 1999), (Haritaoglu et al., 2000), or motion analysis (L. Wang and Tan, 2003). The computational approaches to deal with blob extraction has been essentially developed for gray-level images (Lindeberg and Eklundh, 1991), where the laplacian filtering is the basis to extract image blobs. However, not such an effort has been done to extend this theory to colour images, and usually, the extension is done by just applying the gray-level algorithms on each colour channel separately. Hence the final detection of blobs is the combination of the blobs detected separately on each colour channel, usually red, green and blue. However, in figure 1 we can see that detecting blobs in RGB channels separately, does not assure to get the blobs we perceive in the colour image, in this case we can see small non-elongated blobs in red, yellow, light blue and dark blue, whereas in the RGB channels we have long elongated blobs in different orientations.

The results of this work are framed in the context of a project on automatic image annotation, where one of the goals is the description of textures. There are different approaches to extract and describe texture information and several works discuss how to deal with coloured texture (Maempaa, 2004). A type of approaches are those that build the texture description based on the attribute of its blobs, following psychophysical theories (Julesz and Bergen, 1983). These are the ones that motivates the goal of this paper, that is, to build a colour space that provide an adequate representation to detect colour image blobs as the basis for colour-texture description.

To this end, this paper has been organized as follows. In section 2 we introduce an algorithm to extract the essential colour information of an image, that is, the ridges of the colour distribution. Afterwards, in section 3 we propose a procedure to build a new colour space based on these essential ridges. In section 4 we propose three different criteria to reduce the number of dimensions of this new space, using a statistical measure, a distance-based method or a high-level assumption, being first and second method applied with a constraint satisfaction algorithm. Results and application are showed in 5. Finally, we sum up the conclusions and explain different lines of research.

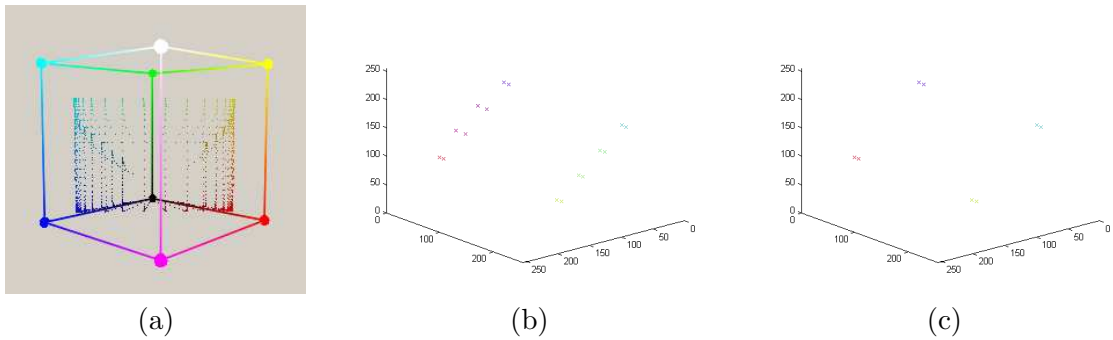


Figure 2: 3D coloured representation of the colour distribution of image 1, (b) ridges detected in the 4D colour distribution and (c) selected ridges

2. Colour-Content Structure

In order to be able to define a colour space with the properties we have expressed above, we will need to extract the essential information of the image content. To this end we will extract this information dealing with the results of a recent work from (E.Vazquez et al., 2007) where they propose to cope the essential colour structure of an image by extracting the ridges (López et al., 2000) of the 3D colour distribution by applying the next formulation, based on the divergence of the structural tensor.

$$\hat{\kappa}_d = -\frac{d}{r} \sum_{k=1}^r \hat{w}_k^t n_k \quad (1)$$

where d is the dimensionality, r is the number of neighbours, n_k is the normal vector of one point, and \hat{w}_k are the dominant directions of that point.

Figure 2.(b) gives the ridges detected by the method from the original image in figure 1 and in figure 2.(c) we show a simplification after removing the noisy ridges as we will explain in next section. This reduction let us to represent the four principal colours we perceive in the original image, these are red, yellow, dark blue and light blue.

It has been proved in (E.Vazquez et al., 2007) that ridges fulfill two essential properties which are those who allow them to cope the colour structure, these are:

- Connectivity of all the points in a ridge.
- Peak and valley substraction, since the ridges extract all the distribution maxima plus all their nearby important colour.

Therefore, we will use this reduced representation of the essential image colour as the basis, in some sense, of our proposal for a new space.

3. Content-Based Colour Space: Definition

In order to compute our proposal for a content-based colour space (CBCS), we must firstly decide the desirable conditions our space should fulfill (J.Vazquez et al., 2007).

Perceptual-coherence: Distances in this space should correlate with perceived colour differences.

Spatial-coherence: Important blobs must maintain its perceived geometric structure.

Chromatic-coherence: Each space dimension should represent a different colour property in order to cope with most of the color information.

Once we have defined these conditions to fulfill, we propose a colour space whose dimension will coincide with the number of important ridges we extract. Therefore, each image channel will be related to a specific ridge.

Let $I : D_I \rightarrow \mathfrak{R}^3$ an image where $D_i \in \mathfrak{R}_+^2$ and $H(I) : \mathfrak{R}^3 \rightarrow \mathfrak{R}$ the image histogram. Let $\{C_k\}_{k=1:m}$ the ridges we extract applying the method introduced in section 2 in $H(I)$.

Let $c_{i,j} \in C_i = \{c_{i,l}\}_{l=1:m'}$ a point that accomplishes

$$\forall x \in C_i \setminus \{c_{i,j}\} \implies H(x) \leq H(c_{i,j}) \quad (2)$$

We will refer $c_{i,j}$ as the ridge-representant. It can be defined in some other ways, for example taking the point that have 50 % of information in each side of the ridge.

Let $d : \mathfrak{R}^n \rightarrow \mathbb{R}$ the Euclidean distance defined as:

$$d(x, y) = \sqrt{\sum_{i=1:n} (x_i - y_i)^2} \quad (3)$$

where $x, y \in \mathfrak{R}^n$. Let $p, q \in D_I$ pixels of the image I . Then we define the new space given by the following image transform $CBCS : D_I \rightarrow \mathfrak{R}^m$ as the space that pixel p in the i -th component has the value:

$$CBCS_i(p) = \max_{q \in D_I} (d(c_{i,j}, I(q))) - d(c_{i,j}, I(p)) \quad (4)$$

At this point, an inverse transform to the original space can be built if we store a little extra information as we explain below. Nevertheless, if we want to re-arrange the values of our channel in a $[0, Y_m]$ range, where Y_m is the maximum intensity value, we must also save the maximum value of our original channel to reconstruct the original image.

Another important consideration is that our space is now defined with a 3D origin. It means that we can take as original image, one in any of the 3D spaces as RGB or CIELAB. Furthermore, to extend our space to other dimensions it would be needed the extension of the ridges extraction algorithm, but all the formulation it would be still true.

The definition we have presented above to build the CBCS space is based on the assumption we have previously selected a reduced set of ridges, in order to have the same number of channels for all the images. To reduce the number of ridges we will use to represent the CBCS we apply a preprocessing step on the ridges obtained with the algorithm of section 2. It is based on an iterative process that reduces those ridges containing a minimum number of pixels in its influence zone (where influence zones are computed from the Voronoi diagram of the ridges on the colour distribution. The original-space values, for instance RGB or CIELAB, of an image point will determine to which influence zone it belongs). Afterwards all these points are redistributed to the remaining ridges. This is

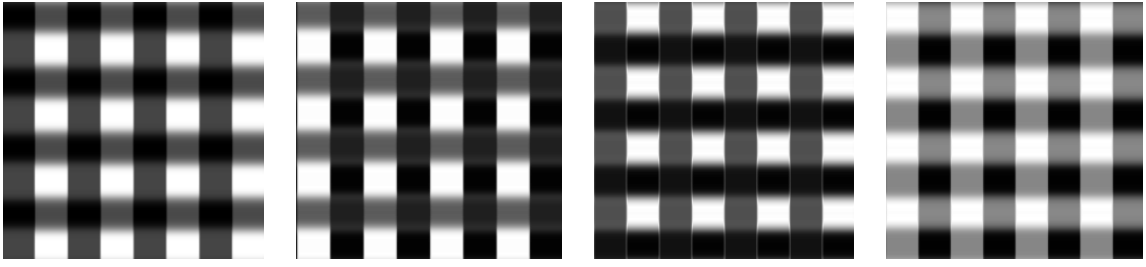


Figure 3: CBCS channels from image in figure 1

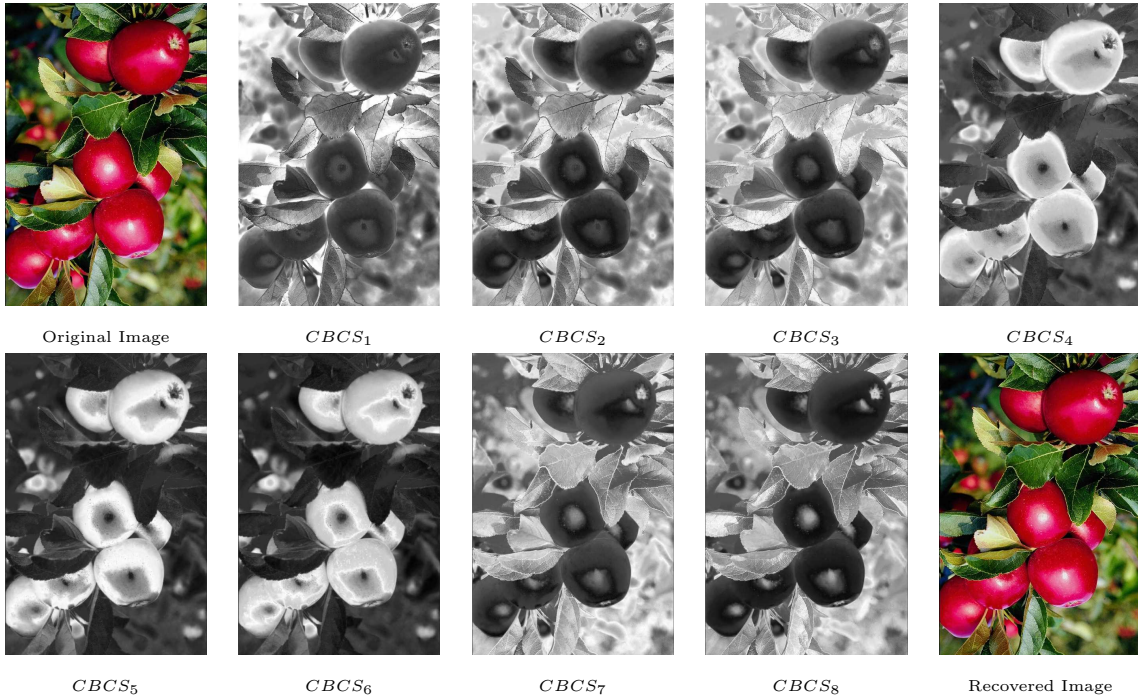


Figure 4: From an original image, its CBCS channels and the image recovered.

repeated iteratively until we achieve a prefixed number of ridges that will be the number of channels of our proposed colour space. The number of ridges we select will determine the amount of information we are able to represent and this number will allow to fulfill the property 3 we have established.

Some results of our space can be showed in figures 3 and 4. In figure 3 we can see the result of applying our space finding the four colours in the original image of figure 1, this means that in each channel we will find the dark blue, red, light blue and yellow blobs respectively. And, in figure 4 we could see from a natural image, its CBCS channels and the recovered image found with the method we will explain below. Both cases are taking CIELAB as the original image space.

On the other hand, to built the inverse transformation is not a hard work. All is based in the next property:

$$\exists p \in D_I, I(p) = c_{i,j} \Rightarrow \max_{q \in D_I} CBCS_i(q) = \max_{q \in D_I} d(c_{i,j}, q) \quad (5)$$

and also,

$$p \in D_i \Rightarrow \min_{q \in D_I} CBCS_i(q) = 0 \quad (6)$$

It is for this that we can say that

$$d(c_{i,j}, p) = \max_{q \in D_I} (CBCS_i(q)) - CBCS_i(p) \quad (7)$$

Once we have this property two different ways of recover the space appear. First one, that minimizes the cost, is to save only three different ridge-representants and make a triangularization from them. Second one, that minimizes the time execution is based in the spherical space since

$$r^i(p) = d(c_{i,j}, p), \quad (8)$$

where r^i is the radius of an sphere centred in c_j that has p has a point. This means that if we compute for one ridge the azimuth and the zenith for each radius, we find an inverse transformation as we will. This transformation is, from cartesian to spherical

$$\begin{aligned} r^i &= \sqrt{x^2 + y^2 + z^2} \\ \theta &= \arctan\left(\frac{y}{x}\right) \\ \phi &= \arccos\left(\frac{z}{r}\right) \end{aligned} \quad (9)$$

And from spherical to cartesian

$$\begin{aligned} x &= r^i \cos \theta \cos \phi \\ y &= r^i \cos \theta \sin \phi \\ z &= r^i \sin \theta \end{aligned} \quad (10)$$

4. Dimensional Reduction

As we have enumerate in section 3, there are three properties we should accomplish. This section is focussed in reaching the Chromatic-coherence, that pursuit to achieve the maximum dissimilarity between channels. To this end we will use three different criteria, a statistical method, a distance-based method and a high-level method. Two first criteria do not provide with an automatic channel-dimension selection, we just apply a Constraint Satisfaction Algorithm with a fixed predefined number of dimensions. On the other hand, third criteria give us the number of channels and which are the preferred channels.

In the first criteria, the constraint we use to sort the channels is based on the mutual information (Karmeshu, 2003).

$$I(X, Y) = H(X) + H(Y) - H(X, Y) \quad (11)$$

where $H(X)$ is the entropy defined as:

$$H(X) = - \sum_{x \in V_x} p(x) * \log_2 p(x) \quad (12)$$

and $H(X, Y)$ is the joint entropy defined as

$$H(X, Y) = - \sum_{x \in V_x} \sum_{y \in V_y} p(x, y) * \log_2 p(x, y) \quad (13)$$

Mutual information is a technique quite used in information theory to make variables to be as independent as they can be. In our case, we select the channels that minimize it, because minimize mutual information is equivalent to maximize independency. To do this minimization we do not use the mutual information explained above, we use a normalized version that is always between 1 and 2 (1 if the channels are independent, 2 if they are dependent) (Hajnal et al., 2001):

$$S(X, Y) = \frac{H(X) + H(Y)}{H(X, Y)} = \frac{H(X) + H(Y)}{H(X) + H(Y) - I(X, Y)} = \frac{I(X, Y)}{H(X, Y)} + 1; \quad (14)$$

To minimize it, we apply a constraint satisfaction algorithm that is an algorithm technique to find the optimal solution fulfilling a set of constraints. It is based on a tree search technique. In our case, we will use a tree of depth n to find the best solution in dimension n . In this case, the constraint to minimize in depth s is:

$$F(a_1, \dots, a_s) = \sum_{i=1:s, j=1:s, i>j} S(a_i, a_j) \quad (15)$$

where $(a_1, \dots, a_s) \in A$, $A = (a_1, \dots, a_m)$ is the set of channels.

Results on this criteria from image in figure 4 are showed in Tables 1 and 2. In the first one we can see the values of the normalized mutual information between all the channels and in the second one, we can see the channels selected by the Constraint Satisfaction algorithm. This criteria seems to performs quite well in selecting channels quite different in each level. In this case, the result for dimension 3 seems to be enough since we find the red apples, the leaves and the background, one in each channel, this is adequate to follows with a blob detection step.

The second criteria is based on the assumption that two similar channels must present less distance that two further channels. It is for this that we define the distance between channels as:

$$d(CBCS_i, CBCS_j) = \sqrt{\frac{\sum_{p \in D_i} (CBCS_i(p) - CBCS_j(p))^2}{\#D_I}} \quad (16)$$

When we have defined this distance we could apply the constraint satisfaction algorithm that maximize the distance between channels. It means to maximize:

$$F(a_1, \dots, a_s) = \sum_{i=1:s, j=1:s, i>j} d(a_i, a_j) \quad (17)$$

	$CBCS_1$	$CBCS_2$	$CBCS_3$	$CBCS_4$	$CBCS_5$	$CBCS_6$	$CBCS_7$	$CBCS_8$
$CBCS_1$	2	1.2958	1.2049	1.1257	1.0984	1.0962	1.1658	1.177
$CBCS_2$	1.2958	2	1.3006	1.1329	1.1129	1.1128	1.1894	1.1908
$CBCS_3$	1.2049	1.3006	2	1.1394	1.1215	1.1297	1.2068	1.1857
$CBCS_4$	1.1257	1.1329	1.1394	2	1.2444	1.2219	1.1364	1.1524
$CBCS_5$	1.0984	1.1129	1.1215	1.2444	2	1.3037	1.1234	1.1312
$CBCS_6$	1.0962	1.1128	1.1297	1.2219	1.3037	2	1.1279	1.1333
$CBCS_7$	1.1658	1.1894	1.2068	1.1364	1.1234	1.1279	2	1.2583
$CBCS_8$	1.177	1.1908	1.1857	1.1524	1.1312	1.1333	1.2583	2

Table 1: Normalized mutual information values to apply the Constraint Satisfaction Algorithm

Dimension	Channels selected
2	$CBCS_1, CBCS_6$
3	$CBCS_1, CBCS_5, CBCS_7$
4	$CBCS_1, CBCS_4, CBCS_6, CBCS_7$
5	$CBCS_1, CBCS_3, CBCS_4, CBCS_6, CBCS_7$
6	$CBCS_1, CBCS_3, CBCS_4, CBCS_5, CBCS_6, CBCS_7$
7	$CBCS_1, CBCS_3, CBCS_4, CBCS_5, CBCS_6, CBCS_7, CBCS_8$

Table 2: Channels selected in each dimension applying mutual information from image in figure 4

	$CBCS_1$	$CBCS_2$	$CBCS_3$	$CBCS_4$	$CBCS_5$	$CBCS_6$	$CBCS_7$	$CBCS_8$
$CBCS_1$	0	26.8552	47.4058	101.8697	120.5651	123.0601	87.7351	85.4542
$CBCS_2$	26.8552	0	23.9958	114.8892	132.9074	136.2849	74.5125	73.6196
$CBCS_3$	47.4058	23.9958	0	119.8127	137.1281	141.2671	59.7812	62.7544
$CBCS_4$	101.8697	114.8892	119.8127	0	27.2009	32.7925	116.757	118.6836
$CBCS_5$	120.5651	132.9074	137.1281	27.2009	0	16.8895	127.9755	129.0985
$CBCS_6$	123.0601	136.2849	141.2671	32.7925	16.8895	0	131.9352	131.6465
$CBCS_7$	87.7351	74.5125	59.7812	116.757	127.9755	131.9352	0	21.8582
$CBCS_8$	85.4542	73.6196	62.7544	118.6836	129.0985	131.6465	21.8582	0

Table 3: Distance values to apply the Constraint Satisfaction Algorithm

Dimension	Channels selected
2	$CBCS_3, CBCS_6$
3	$CBCS_2, CBCS_6, CBCS_7$
4	$CBCS_2, CBCS_5, CBCS_6, CBCS_7$
5	$CBCS_1, CBCS_3, CBCS_5, CBCS_6, CBCS_8$
6	$CBCS_1, CBCS_3, CBCS_5, CBCS_6, CBCS_7, CBCS_8$
7	$CBCS_1, CBCS_3, CBCS_4, CBCS_5, CBCS_6, CBCS_7, CBCS_8$

Table 4: Channels selected in each dimension applying distance between channels from image in figure 4

where $(a_1, \dots, a_s) \in A$, $A = (a_1, \dots, a_m)$ is the set of channels.

Results on this criteria for image 4 are showed in Tables 3 and 4 .In the first one, we could see the distance values between the channels and in the second the channels selected by this method. In dimension 3 we could see that chosen channels are 2, 6 and 7 that are a good representation of the image.

The third criteria is based on the nameability, that has been defined as the ability of assigning a name to a given colour (Tous, 2006) and (Benavente et al., 2004). To apply this criteria we have defined a nameability function of a channel, that is directly related to the nameability function of its associated ridge and this function is defined as follows:

$$N(C_i, j) = \frac{\sum_{r_k \in C_i} (\mu_j(r_k))}{\#C_i} \quad (18)$$

where μ_j is the membership function to give the name j the color r_k and C_i is a ridge. And for each ridge we choose the colour that maximizes equation 18 , it means:

$$\langle v_{name} \rangle_i = (N_{max}, j_{max}) \quad (19)$$

where $N_{max} = \max_{j \in Names} N(C_i, j)$ and j_{max} is the name of the colour where this maximum is reached.

When we have this information of each channel we reduce dimension by removing names repetition, it means, we choose the ridge with high N_{max} for each different j_{max} , or by removing diffused ridges, where a diffused ridge is a ridge that do not have a predominant colour, it means a ridge where the N_{max} is less than a threshold for example we can define a threshold of 0.66.

As a example of this criteria, we can see in Table 5 that from image in figure 4 channels 4, 5 and 6 are mainly red being channel 5 the one with highest N_{max} of them, channels 2, 3, 7 and 8 are green being 3 the highest and channel 1 is mainly black. This means that according to this criteria we select channels 1, 3 and 5.

5. Results and applications

Since the work we are presenting is just a preliminary work in a new research line we are starting to explore, we do not present yet an exhaustive validation for the results. Then

	Red	Orange	Brown	Yellow	Green	Blue	Purple	Pink	Black	Grey	White
$CBCS_1$	0.0003	0	0.0009	0	0.2555	0.0001	0.0006	0	0.7428	0	4.797e-11
$CBCS_2$	4.377e-12	0	0.0002	0	0.9998	4.306e-14	0	0	0	0	0
$CBCS_3$	2.954e-22	0	0	0	1	1.834e-16	1.780e-11	0	0	0	0
$CBCS_4$	0.894	0	0.106	0	6.543e-18	7.865e-24	1.418e-12	0	0	0	0
$CBCS_5$	1	0	4.3e-14	0	2.120e-20	5.930e-31	1.158e-26	0	0	0	0
$CBCS_6$	0.7281	0	4.459e-12	0	1.935e-28	1.535e-25	7.142e-13	0.2719	0	0	0
$CBCS_7$	1.565e-11	0.0002	0	0.0018	0.9982	4.249e-12	1.783e-41	2.646e-14	0	0	0
$CBCS_8$	0	0.0002	0	0.0001	0.9999	0	6.934e-13	0	0	0	0

Table 5: Results of the Nameability function in figure 4. Once we have this we want to take the maximum for each row to know the colour name of the channel

in this section we will only present a qualitative validation of the results, to extract some conclusions about the feasibility of this new research line.

This section will be divided into two parts. In the first part we will show the CBCS channels computed on different images and the dimensional reduction step. In the second part, we analyze on a set of images the behaviour of the proposed space in the visual task of detecting blobs.

In figures 5,6,7,8 and 9 we can see the $CBCS$ transform for each image and we can also see two tables for each image, one with the results of criterias 1 and 2 (mutual information and distance) of the dimensionality reduction results, and another with the results of criteria 3 (Nameability).

In figure 5 we can see the CBCS channels, that extracts the flowers (in its different chromaticities: channels e,f,g,), the trees (channels a,b,d), the mountains (channel h) and the grass (channel c). If we see tables 6 and 7, we observe that Nameability seems to work as expected, and distance-based method also, but mutual information could be not the best way to solve. On the other hand, we can see in figure 6, table 8, table 9 that in this case channel g does not appear in the distance-method in low dimensions, and this is not a good solution. Other two methods seems to works properly.

In other sense in figure 7, when we see Table 11 it seems to be necessary more colour names because we said as purple two different colours: violet and lilac. The other two methods, that are exposed on Table 10 works correctly and they give us the three interpretations the image need it. In figure 8, the three validation method works properly, as we show in Tables 12 and 13 and also it is quite clear that our colour space brings us a great decomposition of the image. There are mainly 3 interpretations: flowers (channels f,g,h), trucks (d,e) and background (a,b,c) and in all the methods we find them greatly.

To finish this part of the section, in figure 9 we can also see that the different flowers are detected, and the channels represents quite well the image. The results of the dimensionality reduction step, showed in tables 14 and 15, show us that distance-based method works correctly, Nameability also works correctly, but it can be interesting to consider two different greens, and mutual information works well too, but not as well as the others two, because yellow flowers appear in dimension 5. All the results in these images have been done applying our method in the CIELAB space.



Figure 5: CBCS channels from an original image. In Tables 6 and 7 we can see the dimensionality reduction of these channels with each method

Dimension	Channels selected by mutual information	Channels selected by distance
2	e,h	b,f
3	c,e,h	a,f,h
4	c,e,g,h	a,f,g,h
5	c,d,e,g,h	b,c,f,g,h
6	a,c,d,e,g,h	a,b,e,f,g,h
7	a,c,d,e,f,g,h	a,c,d,e,f,g,h

Table 6: Dimensionality reduction with criteria 1 and 2 from figure 5

Channel	j_{max}	N_{max}	Selected?
a	Green	1	Yes (this one or c)
b	Green	0.9996	No (a and c have higher N_{max})
c	Green	1	Yes (this one or a)
d	Blue	0.5095	No (Diffused ridge)
e	Brown	0.5301	No (Diffused ridge)
f	Red	0.951	Yes
g	Orange	0.5526	No (Diffused ridge)
h	Blue	0.9924	Yes

Table 7: Dimensionality reduction with criteria 3 from figure 5

Dimension	Channels selected by mutual information	Channels selected by distance
2	d,g	c,e
3	a,d,g	b,e,h
4	a,d,f,g	c,d,e,h
5	a,d,f,g,h	a,c,d,e,h
6	a,d,e,f,g,h	a,c,d,e,g,h
7	a,c,d,e,f,g,h	a,c,d,e,f,g,h

Table 8: Dimensionality reduction with criteria 1 and 2 from figure 6

Channel	j_{max}	N_{max}	Selected?
a	Black	0.6243	No (Diffused ridge)
b	Green	0.8967	No (c has higher N_{max})
c	Green	0.9933	Yes
d	Red	0.7837	Yes
e	Orange	0.9993	Yes
f	Green	0.7622	No (c has higher N_{max})
g	Yellow	0.9969	Yes
h	Blue	0.9865	Yes

Table 9: Dimensionality reduction with criteria 3 from figure 6

Dimension	Channels selected by mutual information	Channels selected by distance
2	a,f	d,e
3	a,f,g	a,d,h
4	a,b,f,g	a,d,e,g
5	a,b,f,g,h	a,c,d,e,h
6	a,b,c,f,g,h	a,b,d,e,g,h
7	a,b,c,e,f,g,h	a,b,c,d,e,g,h

Table 10: Dimensionality reduction with criteria 1 and 2 from figure 7

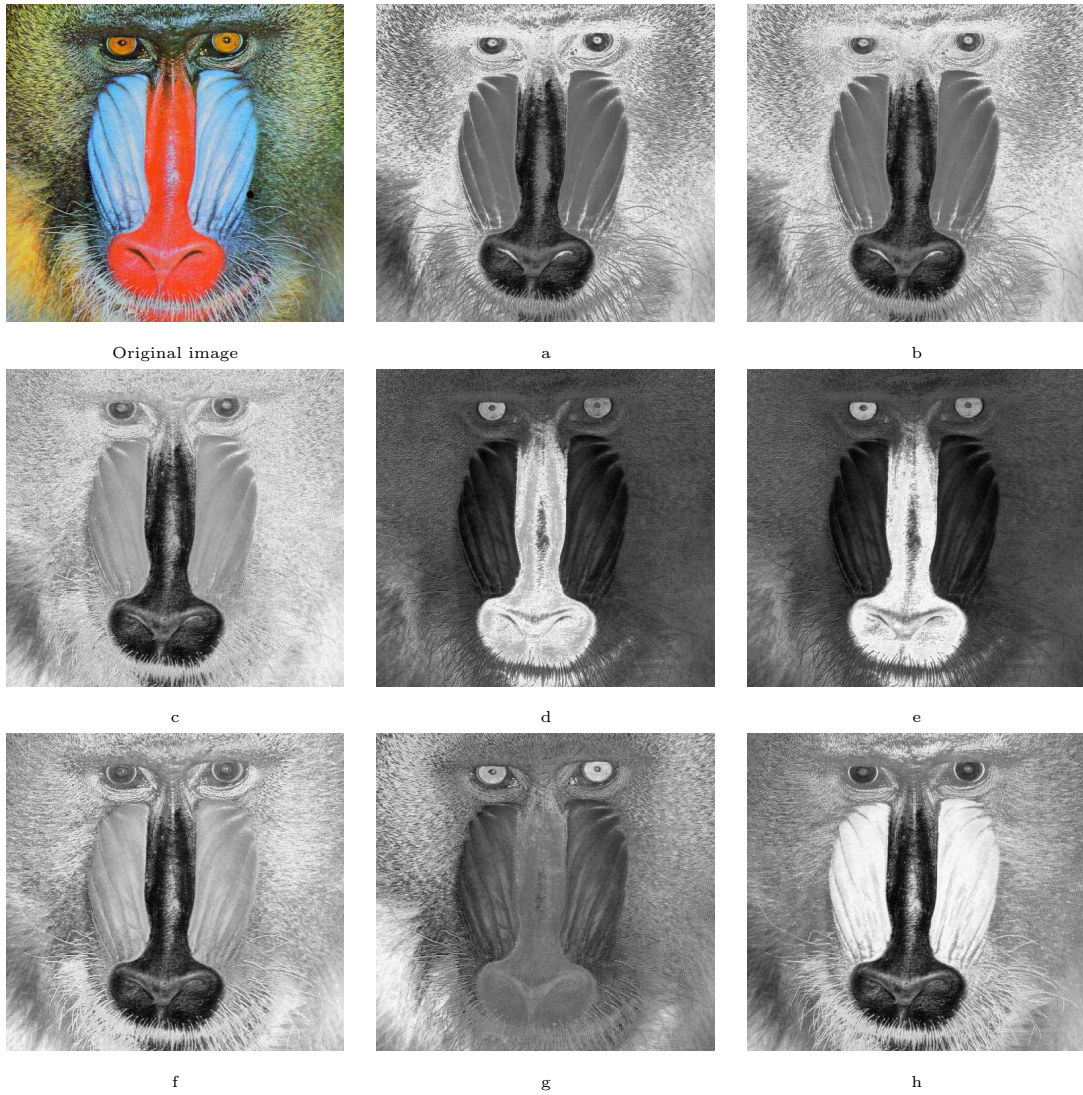


Figure 6: CBCS channels from an original image. In Tables 8 and 9 we can see the dimensionality reduction of these channels with each method

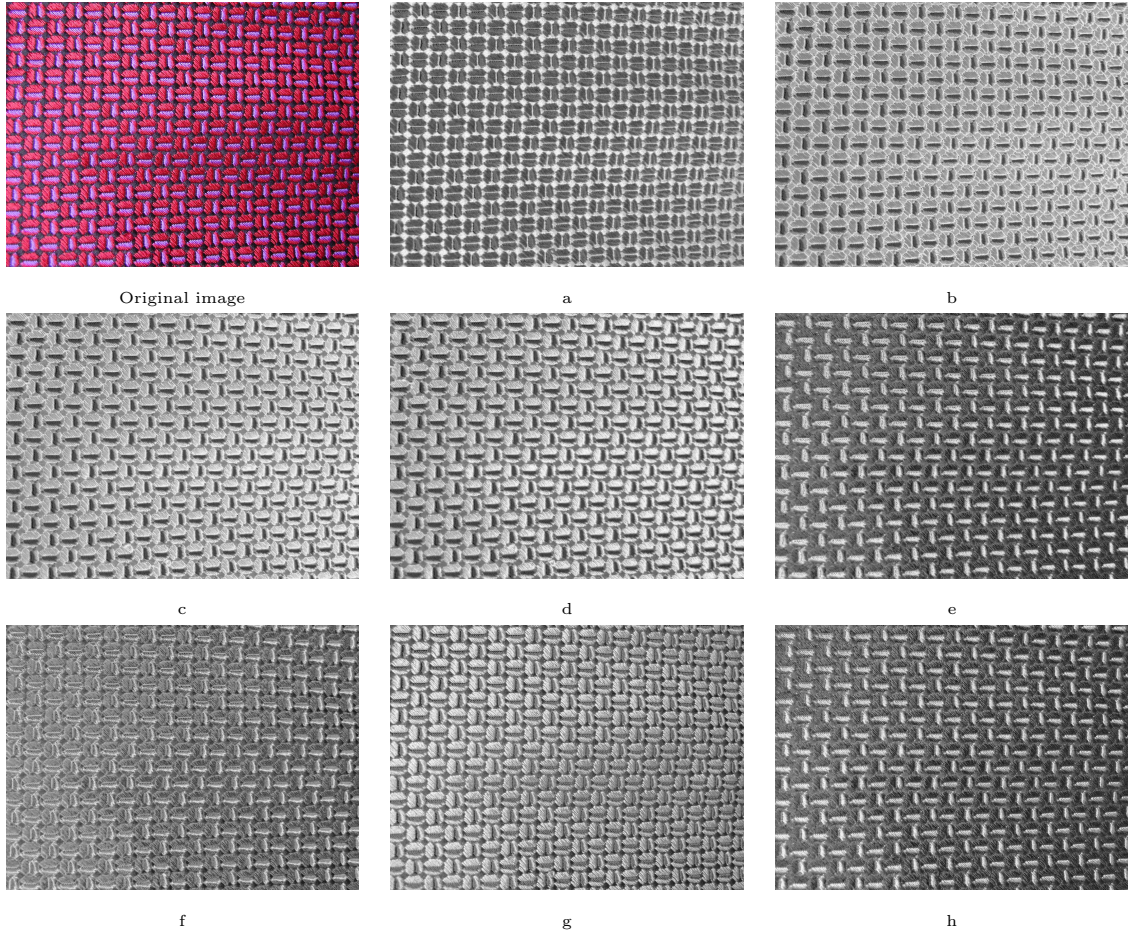


Figure 7: CBCS channels from an original image. In Tables 10 and 11 we can see the dimensionality reduction of these channels with each method

Channel	j_{max}	N_{max}	Selected?
a	Purple	0.9412	No (e has higher N_{max})
b	Red	0.8908	No (c has higher N_{max})
c	Red	0.9999	Yes
d	Red	0.9647	No (c has higher N_{max})
e	Purple	1	Yes
f	Purple	0.5369	No (Diffused ridge)
g	Pink	1	Yes
h	Purple	0.9967	No (e has higher N_{max})

Table 11: Dimensionality reduction with criteria 3 from figure 7

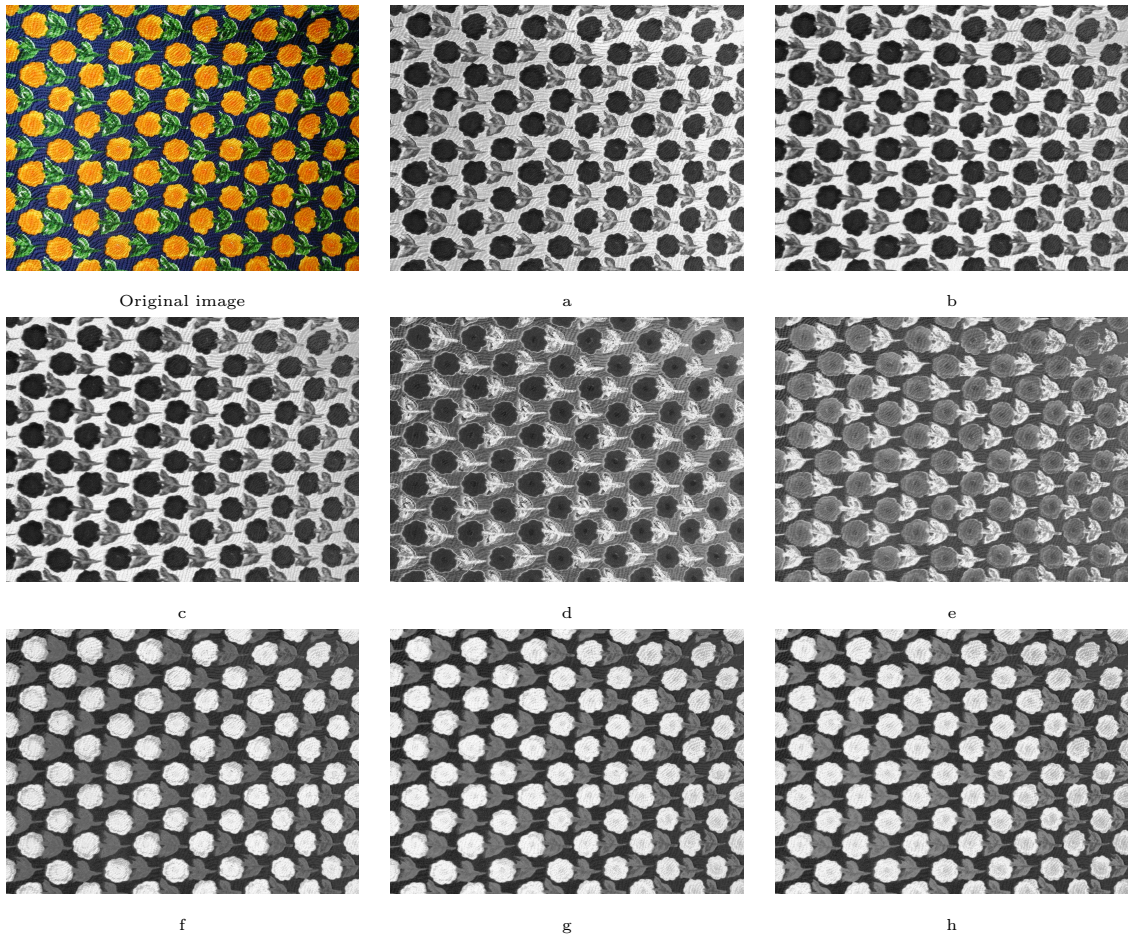


Figure 8: CBCS channels from an original image. In Tables 12 and 13 we can see the dimensionality reduction of these channels with each method

Dimension	Channels selected by mutual information	Channels selected by distance
2	a,d	b,g
3	a,d,e	b,d,g
4	a,d,e,f	a,c,f,g
5	a,c,d,e,f	b,c,d,f,g
6	a,c,d,e,f,h	a,b,c,e,f,g
7	a,b,c,d,e,f,h	a,b,c,d,f,g,h

Table 12: Dimensionality reduction with criteria 1 and 2 from figure 8

Channel	j_{max}	N_{max}	Selected?
a	Black	0.7374	Yes
b	Blue	0.9932	No (c has higher N_{max})
c	Blue	0.9974	Yes
d	Green	1	Yes (or e)
e	Green	1	Yes (or d)
f	Orange	0.9908	Yes
g	Orange	0.9214	No (f has higher N_{max})
h	Yellow	0.996	Yes

Table 13: Dimensionality reduction with criteria 3 from figure 8

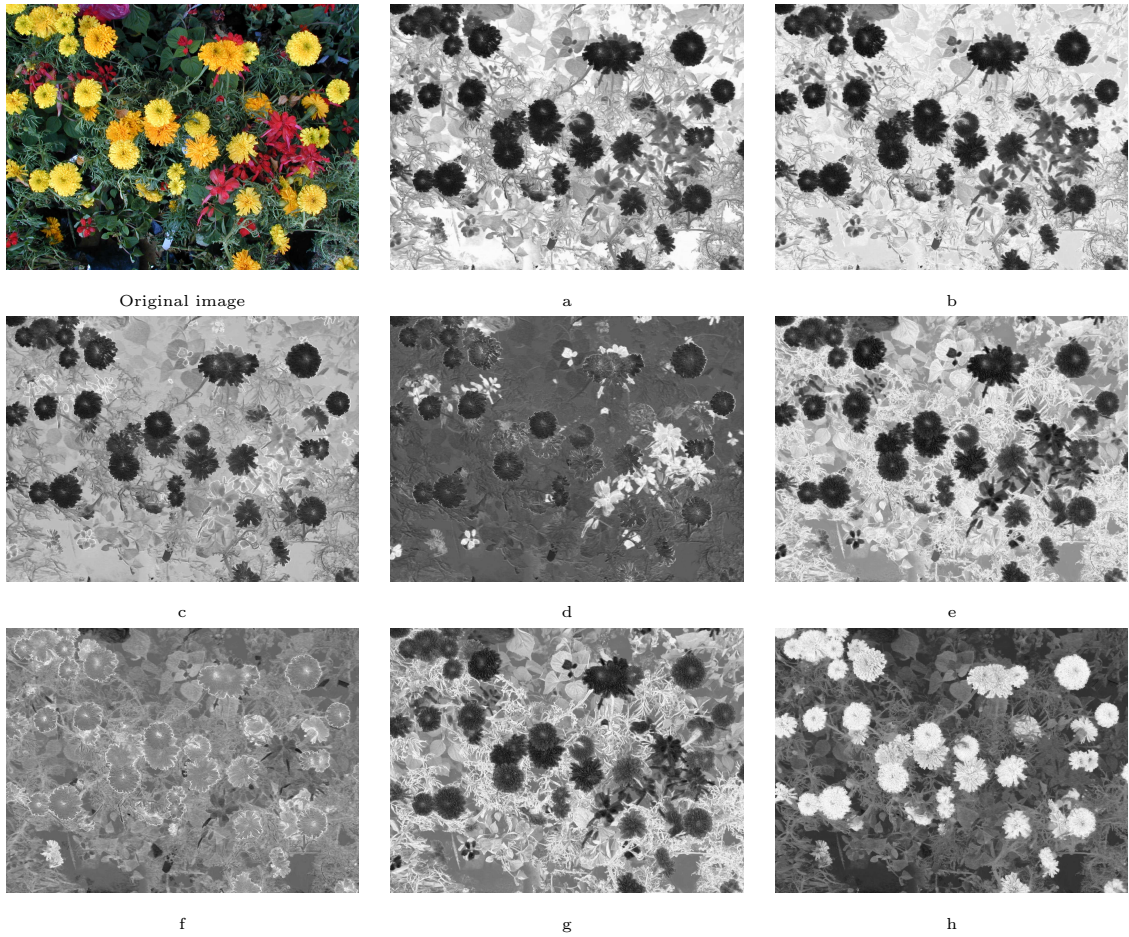


Figure 9: CBCS channels from an original image. In Tables 14 and 15 we can see the dimensionality reduction of these channels with each method

Dimension	Channels selected by mutual information	Channels selected by distance
2	d,f	b,h
3	d,f,g	b,d,h
4	c,d,f,g	b,d,e,h
5	c,d,f,g,h	a,b,d,g,h
6	b,c,d,f,g,h	a,b,d,e,f,h
7	b,c,d,e,f,g,h	a,b,d,e,f,g,h

Table 14: Dimensionality reduction with criteria 1 and 2 from figure 9

Channel	j_{max}	N_{max}	Selected?
a	Black	0.9936	Yes
b	Green	0.9995	Yes
c	Red	0.9711	No (d has higher N_{max})
r	Red	0.9998	Yes
e	Green	0.9905	No (b has higher N_{max})
f	Brown	0.5038	No (Diffused Ridge)
g	Green	0.8857	No (b has higher N_{max})
h	Yellow	0.8975	Yes

Table 15: Dimensionality reduction with criteria 3 from figure 9

On the other hand, if we try to find an application for our space, the clearest one is the blob detection. In figures 10 and 11 we have applied a blob detection algorithm created by (A.Salvatella et al., 2003) in our space and its RGB.

The results of this comparison could be clearly seen in figure 10, where the RGB channels are practically equal and they only found one of the three different parts of the image. Nevertheless, in the CBCS channels we can find the three different parts of the image. In this image we have applied the method in an RGB image. Moreover, in figure 11 we can see the results of the blob detection algorithm in 8 using the channels chosen by nameability. In this case it is also clear that our space finds out the different parts of the image, but RGB channels do not detect the trunks and the background.

6. Conclusions and Further Work

This preliminary work is based on the assumption that colour and texture are quite related cues, it means that we could not consider one and reject any information of the other. In particular, this work is a first step in the idea of adapting colour information to help texture descriptors based on image blobs.

Nevertheless, although it is a preliminary work, some goals are achieved. One of them is the novelty of the idea, since to consider the coloured blob detection problem from a representational point of view has not been approached yet. Moreover, in this work we have given a first approach to the properties that a space with this objective should accomplish.

We also give an algorithm to compute an space accomplishing these properties, and we propose some criteria to compare the channels contents.

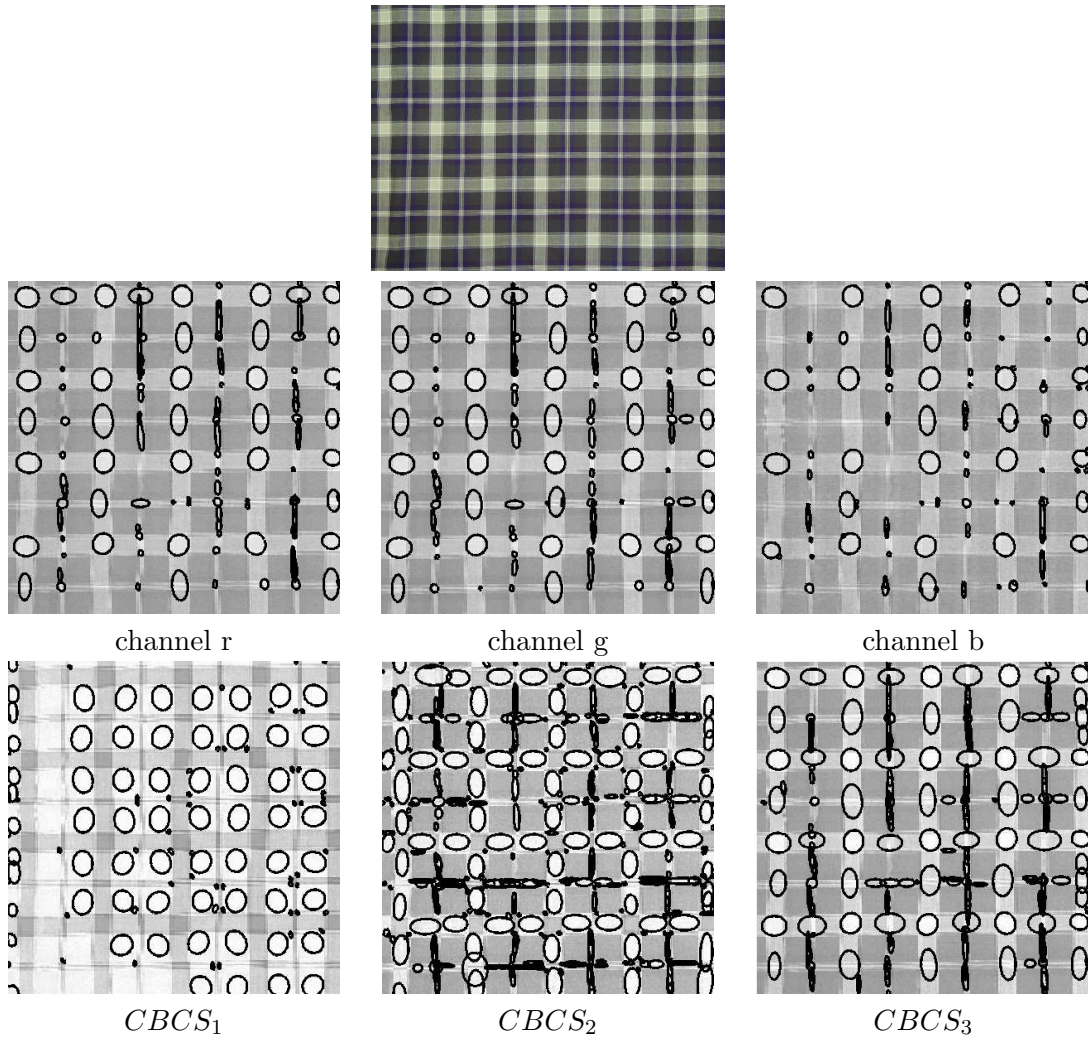


Figure 10: Comparison between blobs detected in RGB from an image and blobs detected in *CBCS*. In this case *CBCS* has been applied taking RGB as the original space (in all of the other cases the origin has been CIELAB)

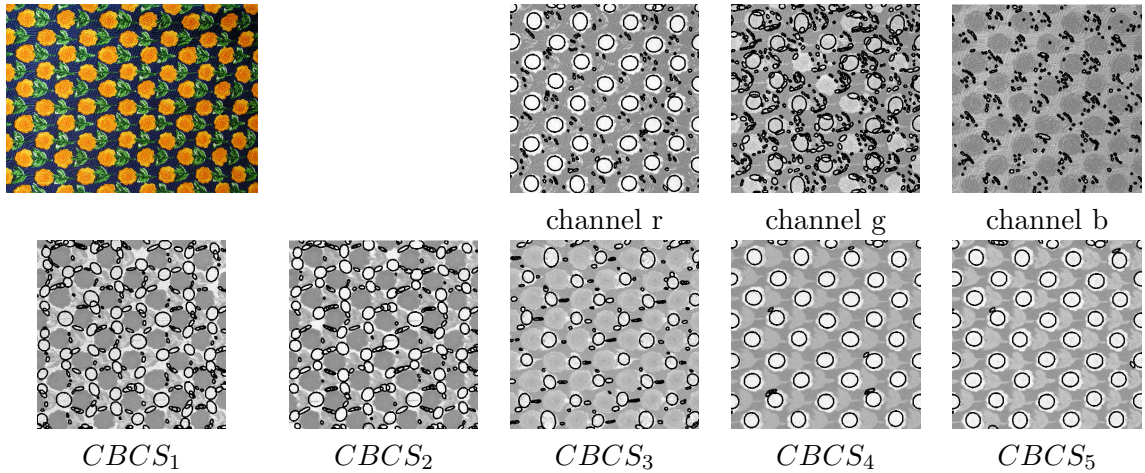


Figure 11: Comparison between blobs detected in CBCS channels of figure 8 selected by Nameability and blobs detected in RGB

As it can be seen in section 5 results are quite encouraging and it seems that this idea could support a new vision on blob detection. It must be also studied some other applications of the space because we think that this space must also be useful in other applications.

There are quite different ways to continue. Clearly a deeper study must be done in the selection step, to improve and combine the different criteria we could consider, three have been explained in this work and others that could appear.

In the same sense we can try to change the Constraint Satisfaction algorithm by a cluster, not to select directly the channels, but to join them in some sets that represent more or less the same part of the image.

We also would try to make *CBCS* independent to the illuminant. This could imply makes some changes on the ridges or to introduce new features. But we think that is an important step towards a complete and useful colour space.

Finally, it must be also important to prove our space in a complete and specialized database, to detect some other weaknesses and improve them.

Acknowledgments

This project have been partially supported by MEC TIN2004-02970
 "AUTOMATIC TEXTUAL ANNOTATION ON IMAGE DATABASES BASED ON VISUAL DESCRIPTORS COMBINING SPATIO-CHROMATIC INFORMATION"

References

A.Salvatella, M.Vanrell, and R.Baldrich. Subtexture components for texture description. *1st. Iberian conference on Pattern Recognition and Image Understanding-ibPRIA'2003,LNCS 2652:884-892*, 2003.

- R. Benavente, M. Vanrell, and R. Baldrich. Estimation of fuzzy sets for computational colour categorization. *Color Research and Application*, 29(5):342–353, 2004.
- H.D. Cheng, X.H. Jiang, Y. Sun, and J. Wang. Color image segmentation: advances and prospects. *Pattern Recognition*, 34(6):2259–2281, 2001.
- R. Collins, A. Lipton, and T. Kanade. A system for video surveillance and monitoring. In *American Nuclear Society 8th Internal Topical Meeting on Robotics and Remote Systems*, 1999. URL citeseer.ist.psu.edu/article/collins99system.html.
- N. Dominy and P. Lucas. Ecological importance of trichromatic vision to primates. *Nature*, 410:363–366, 2001.
- E. Vazquez, Ramon Baldrich, Javier Vazquez, and Maria Vanrell. Topological histogram reduction towards colour segmentation. *4477-0055 - Lecture Notes in Computer Science - Pattern Recognition and Image Analysis*, 2007.
- J. Hajnal, D. Hill, and D. Howkes. *Medical Images Registration*. CRC Press, 2001.
- Ismail Haritaoglu, Davis Harwood, and Larry S. David. W4: Real-time surveillance of people and their activities. *IEEE Trans. Pattern Anal. Mach. Intell.*, 22(8):809–830, 2000. ISSN 0162-8828. doi: <http://dx.doi.org/10.1109/34.868683>.
- B. Julesz and J.R. Bergen. Textons, the fundamental elements in preattentive vision and perception of textures. *Bell Systems Technological Journal*, 62:1619–1645, 1983.
- J. Vazquez, Maria Vanrell, Anna Salvatella, and Eduard Vazquez. A colour space based on the image content. In *Frontiers on Artificial intelligence*. IOS Press, 2007.
- Karmeshu. *Entropy measures, maximum entropy Principle and emerging Applications*. Springer, 2003.
- W. Hu L. Wang and T. Tan. Recent developments in human motion analysis. *Pattern Recognition*, 36(3):585,601, 2003.
- T. Lindeberg and Jan-Olof Eklundh. On the computation of a scale-space primal sketch. *Journal of Visual Communications and Image Representation*, 2(1):55–78, 1991.
- Antonio M. López, David Lloret, Joan Serrat, and Juan J. Villanueva. Multilocal creaseness based on the level-set extrinsic curvature. *Computer Vision and Image Understanding: CVIU*, 77(2):111–144, February 2000. ISSN 1077-3142. doi: 10.1006/cviu.1999.0812.
- Tolhurst D. J. Parraga C. A. Baddeley R. Leonards U. Lovell, P. G. and J. Troscianko.
- Pietikaainen Maempaa, T. Classification with color and texture: jointly or separately? *Pattern Recognition*, 37:1629–1640, 2004.
- JD Mollon. "Tho' she kneel'd in that place where they grew..." The uses and origins of primate colour vision. *J Exp Biol*, 146(1):21–38, 1989. URL <http://jeb.biologists.org/cgi/content/abstract/146/1/21>.

Troscianko T. Parraga C.A. and Tolhurst D.J. Spatiochromatic properties of natural images and human vision. *Current Biology*, 12(6):483–487(5), 2002.

Francesc Tous. *Computational framework for the white point interpretation based on colour matching*. PhD thesis, Computer Vision Center, 2006.

G. Wyszecki and W.S. Stiles. *Color science: concepts and methods, quantitative data and formulae*. John Wiley & Sons, 2nd edition, 1982.